Original Article | Gastrointestinal Imaging

eISSN 2005-8330
https://doi.org/10.3348/kjr.2023.1235
Korean J Radiol 2024;25(7):644-655

Korean Journal of Radiology
KJR

Predicting Recurrence-Free Survival After Upfront Surgery in Resectable Pancreatic Ductal Adenocarcinoma: A Preoperative Risk Score Based on CA 19-9, CT, and ^{18}F-FDG PET/CT

Boryeong Jeong[1]*, Minyoung Oh[2]*, Seung Soo Lee[1], Nayoung Kim[3], Jae Seung Kim[2], Woohyung Lee[4], Song Cheol Kim[4], Hyoung Jung Kim[1], Jin Hee Kim[1], Jae Ho Byun[1]

[1]Department of Radiology and Research Institute of Radiology, University of Ulsan College of Medicine, Asan Medical Center, Seoul, Republic of Korea
[2]Department of Nuclear Medicine, University of Ulsan College of Medicine, Asan Medical Center, Seoul, Republic of Korea
[3]Department of Clinical Epidemiology and Biostatistics, University of Ulsan College of Medicine, Asan Medical Center, Seoul, Republic of Korea
[4]Division of Hepatobiliary and Pancreatic Surgery, Department of Surgery, University of Ulsan College of Medicine, Asan Medical Center, Seoul, Republic of Korea

Objective: To develop and validate a preoperative risk score incorporating carbohydrate antigen (CA) 19-9, CT, and fluorine-18-fluorodeoxyglucose (^{18}F-FDG) PET/CT variables to predict recurrence-free survival (RFS) after upfront surgery in patients with resectable pancreatic ductal adenocarcinoma (PDAC).

Materials and Methods: Patients with resectable PDAC who underwent upfront surgery between 2014 and 2017 (development set) or between 2018 and 2019 (test set) were retrospectively evaluated. In the development set, a risk-scoring system was developed using the multivariable Cox proportional hazards model, including variables associated with RFS. In the test set, the performance of the risk score was evaluated using the Harrell C-index and compared with that of the postoperative pathological tumor stage.

Results: A total of 529 patients, including 335 (198 male; mean age ± standard deviation, 64 ± 9 years) and 194 (103 male; mean age, 66 ± 9 years) patients in the development and test sets, respectively, were evaluated. The risk score included five variables predicting RFS: tumor size (hazard ratio [HR], 1.29 per 1 cm increment; $P < 0.001$), maximal standardized uptake values of tumor ≥ 5.2 (HR, 1.29; $P = 0.06$), suspicious regional lymph nodes (HR, 1.43; $P = 0.02$), possible distant metastasis on ^{18}F-FDG PET/CT (HR, 2.32; $P = 0.03$), and CA 19-9 (HR, 1.02 per 100 U/mL increment; $P = 0.002$). In the test set, the risk score showed good performance in predicting RFS (C-index, 0.61), similar to that of the pathologic tumor stage (C-index, 0.64; $P = 0.17$).

Conclusion: The proposed risk score based on preoperative CA 19-9, CT, and ^{18}F-FDG PET/CT variables may have clinical utility in selecting high-risk patients with resectable PDAC.

Keywords: Pancreatic ductal adenocarcinoma; Surgery; Recurrence-free survival; ^{18}F-FDG PET/CT; Carbohydrate antigen 19-9

INTRODUCTION

Pancreatic ductal adenocarcinoma (PDAC) is a highly lethal disease with a five-year survival rate of only 10% [1]. The primary curative option for PDAC is surgical resection; however, resection applies to 20% of PDAC patients who

Received: December 12, 2023 **Revised:** April 11, 2024 **Accepted:** April 12, 2024
*These authors contributed equally to this work.
Corresponding author: Seung Soo Lee, MD, PhD, Department of Radiology and Research Institute of Radiology, University of Ulsan College of Medicine, Asan Medical Center, 88 Olympic-ro 43 gil, Songpa-gu, Seoul 05505, Republic of Korea
• E-mail: seungsoolee@amc.seoul.kr

Korean Journal of Radiology
KJR

have early-stage disease [2]. Even among patients who undergo curative resection, the risk of recurrence remains high, with recurrence rates reaching 50% within one year [2].

Currently, treatment decisions for PDAC are based on anatomical tumor resectability; neoadjuvant therapy has been widely accepted as the initial treatment for borderline resectable or locally advanced PDAC [3,4]. For resectable PDAC, the standard treatment involves upfront surgery followed by adjuvant therapy. The observed survival benefits of neoadjuvant therapy for borderline resectable PDAC [5] have generated interest in extending its application to patients with resectable PDAC. Practice guidelines suggest the use of neoadjuvant therapy in select high-risk patients with resectable PDAC; however, the criteria for identifying such patients have yet to be clearly defined [3,4].

The recently introduced concept of biological resectability emphasizes considering tumor biology and anatomical resectability when selecting a treatment option [6-11]. Potential tumor biological markers include carbohydrate antigen (CA) 19-9, suspicious lymph node (LN) metastasis, and the maximum standardized uptake value (SUV_{max}) of the tumor on fluorine-18 (^{18}F)-labeled fluorodeoxyglucose (FDG) PET/CT [6]. This concept suggests that anatomically resectable PDAC, which exhibits features of aggressive tumor biology, may be better classified as borderline resectable PDAC. However, the validity of biological resectability requires further investigation. Previous studies evaluating the prognostic role of CA 19-9 and tumor SUV_{max} in PDAC have been limited by factors such as a small sample size [10], lack of independent validation [8,9,11], and insufficient consideration of other findings such as tumor size or anatomical tumor resectability [8,10,11]. Additionally, given the routine use of pancreatic CT for staging, CT findings must be incorporated into selecting high-risk patients with resectable PDAC.

Therefore, the purpose of our study was to develop and validate a preoperative risk-scoring system that incorporates CA 19-9 and clinical, CT, and ^{18}F-FDG PET/CT variables to predict recurrence-free survival (RFS) following upfront surgery in patients with resectable PDAC.

MATERIALS AND METHODS

Our Institutional Review Board approved this retrospective study (IRB No. 2019-0993), which waived the requirement for informed consent. Our study followed the guidelines for transparent reporting of a multivariable prediction model for individual prognosis or diagnosis [12].

Study Population

We retrospectively registered consecutive patients with resectable PDAC at a single tertiary center between January 2014 and December 2019. The inclusion criteria were pathologically proven PDAC according to the 2010 World Health Organization classification [13], resectable PDAC determined on pancreatic protocol CT within one month before surgery, available serum CA 19-9 and ^{18}F-FDG PET/CT findings within two months before surgery, and receipt of curative-intent upfront surgery. Resectable PDAC was defined as a tumor with no major arterial contact and no contact or ≤ 180° contact with the portomesenteric vein without contour deformity according to the national comprehensive cancer network guidelines [14] and the absence of evident metastasis on CT or ^{18}F-FDG PET/CT. Patient eligibility for resectable PDAC was confirmed through a retrospective review of CT images conducted by two board-certified radiologists (B.J. and S.S.L., with 5 and 17 years of experience, respectively). The exclusion criteria were as follows: no visible mass on CT, multiple PDACs, coexisting malignancies within 5 years of PDAC diagnosis, prior pancreatic surgery, and aborted or palliative surgery due to inoperable conditions identified during surgery. The final study population was divided into development (surgery between January 2014 and December 2017) and test (surgery between January 2018 and December 2019) sets based on the date of pancreatic surgery.

Clinical Variables

Demographic and laboratory variables potentially associated with PDAC prognosis were collected [15], including age, sex, body mass index, CA 19-9 levels, albumin, bilirubin, alkaline phosphatase, C-reactive protein, and lymphocyte and platelet counts. CA 19-9 levels obtained in the absence of biliary obstruction or after proper biliary drainage in cases of obstructive jaundice (i.e., bilirubin > 2 mg/dL) were considered evaluable because biliary obstruction causes an artificial increase in CA 19-9 levels [16,17].

CT Examination and Analysis

All patients underwent pancreatic protocol CT as recommended by the practice guidelines [3,4]. The imaging protocol included unenhanced and contrast-enhanced arterial- and portal-venous phase imaging. Arterial and portal venous phase images were reconstructed in axial and

 https://doi.org/10.3348/kjr.2023.1235

coronal planes at 2.5 to 3.0 mm thickness. Details of these techniques are provided in the Supplementary Methods. The same radiologists (B.J. and S.S.L.) who assessed tumor resectability independently reviewed the CT images. They then reached a consensus on tumor location (i.e., head, body, and tail), maximal tumor diameter, adjacent organ invasion, and suspicious regional LN per PDAC radiological reporting template [18] while blinded to clinical information. The criteria for suspicious regional LN were a short-axis diameter > 1 cm, abnormal round morphology, heterogeneity, or central necrosis [18].

^{18}F-FDG PET/CT Examination and Analysis

All patients fasted for at least six hours before ^{18}F-FDG PET/CT examination, and their venous blood glucose level was < 140 mg/dL. ^{18}F-FDG PET/CT examinations were performed using the Biograph Sensation 16 or TruePoint 40 (Siemens, Knoxville, TN, USA) and Discovery 690, 690 Elite, or 710 (GE Healthcare, Milwaukee, WI, USA) scanners, which were routinely calibrated against dose calibrators and well counters. After intravenously injecting 0.14 mCi/kg ^{18}F-FDG, PET/CT images were acquired from the skull base to the upper thigh and reconstructed using an iterative algorithm with attenuation correction. Two board-certified nuclear medicine physicians (J.S.K. and M.O., with 27 and 10 years of experience, respectively) retrospectively analyzed all ^{18}F-FDG PET/CT images in consensus using a dedicated workstation (Syngo.via VB40, Siemens, Erlangen, Germany). The tumor SUV_{max} was measured by drawing a volume of interest encompassing the tumor. Suspicious regional LNs were visually assessed and defined as LNs that showed higher metabolic activity than the liver [19,20]. Possible (but not evident) distant metastasis was defined as an abnormal focal hypermetabolic lesion discernible by physiological uptake.

Surgery and Outcome Measures

The primary outcome was RFS, defined as the time from the surgery date until the recurrence or death. The secondary outcome was overall survival. A multidisciplinary panel including radiologists, oncologists, and surgeons made therapeutic decisions. Surgery was performed by one of five pancreatic surgeons who underwent more than 50 pancreatic cancer surgeries annually. Postoperatively, patients were followed up regularly by clinical evaluation, serum CA 19-9, and CT every 3–6 months until death, their last clinical visit, or the end of the follow-up period (July 2022). Patients with distant metastases identified during surgery and who underwent complete resection of primary and metastatic tumors at the surgeon's discretion were included to avoid selection bias. In these patients, recurrence was recorded when a clinically unequivocal recurrence was detected.

Pathological Findings

We recorded the pathological findings of the surgical specimens, including tumor stage, following the eighth edition of the American Joint Committee on Cancer Staging System [21]; pathological margin status as defined by the British Royal College of Pathology guidelines [22]; and perineural invasion, lymphovascular invasion, and tumor differentiation.

Statistical Analysis

Continuous variables were compared using *t*-tests or Wilcoxon rank-sum tests, and categorical variables were compared using the chi-square test. Inter-reader agreement on CT variables was evaluated using the intraclass correlation coefficient or Fleiss kappa statistics. Suspicious regional LNs evaluated using CT and ^{18}F-FDG PET/CT were combined into a single variable because of their high correlation. They were considered present if suspicious regional LNs were identified on either CT or ^{18}F-FDG PET/CT scans. Missing data were addressed using multiple imputations with the Markov chain Monte Carlo method [23]. We performed a univariable Cox proportional hazard analysis in the development set to evaluate the association between the variables and RFS. For significant continuous variables, we used a restricted cubic spline model [24] to evaluate the linearity of the association with the log relative hazard of recurrence or death. Nonlinear variables were dichotomized at the threshold at which the sum of sensitivity and specificity for predicting 1-year RFS was maximized [25]. A multivariable Cox proportional hazards model was constructed to predict RFS. Variable selection was performed using multivariable Cox proportional hazard analysis with backward elimination conducted using the bootstrapping selection method with 1000 replications [12]. The final prediction model included variables in more than 50% of the bootstrap samples. Subsequently, we developed a risk-scoring system by assigning weighted points to each variable based on the ratio of the regression coefficient to the reference variable rounded to the nearest whole number [26]. The discrimination performance of the risk score was assessed using Harrell's C-index [27,28]. The calibration performance of the risk score was assessed using the calibration plot [29] and calibration slope [30] and

https://doi.org/10.3348/kjr.2023.1235

Korean Journal of Radiology
KJR

by comparing the predicted and observed RFS at one year. Performance was evaluated in the development set (using the optimism-corrected C-index through bootstrapping with 1000 iterations for internal validation of discrimination performance) and the test set. The discrimination performance of the risk score was compared to that of the postoperative pathological tumor stage in the test set [31]. The risk scores were categorized into low- and high-risk groups based on the probability of one-year RFS. Kaplan–Meier survival curves for RFS and overall survival were plotted and compared between the risk groups using the log-rank test. The correlations of tumor SUV_{max} and CA 19-9 with pathological findings were evaluated using the chi-square test or one-way analysis of variance. $P < 0.05$ was considered to indicate statistically significant. All statistical analyses were performed using SPSS version 22 (IBM Corp., Armonk, NY, USA) and R version 4.2.2 (R Foundation for Statistical Computing, Vienna, Austria; https://www.R-project.org).

RESULTS

Patient Characteristics

Of the 577 eligible patients, 48 were excluded because of the absence of a visible mass on CT (n = 5), multiple PDACs (n = 10), coexisting malignancy within 5 years of PDAC diagnosis (n = 24), prior pancreatic surgery (n = 4), or aborted or palliative surgery (n = 5) (Fig. 1). The final study population (529 patients) was divided into the development (n = 335; 198 males; mean age ± standard deviation, 64 ± 9 years) and test (n = 194; 103 males; mean age ± standard deviation, 66 ± 9 years) sets (Fig. 1).

Table 1 summarizes the characteristics of the study population. The RFS (median, 14.6 months vs. 12.0 months; $P < 0.001$) and overall survival (median, 33.6 months vs. 33.0 months; $P < 0.001$) were more extended in the test set than in the development set. All patients underwent curative-intent pancreatic resection, with additional vein resection in 53 (15.8%) and 21 (10.8%) patients and artery resection in 8 (2.4%) and 3 (1.5%) patients in the development and test sets, respectively. Nine (1.7%)

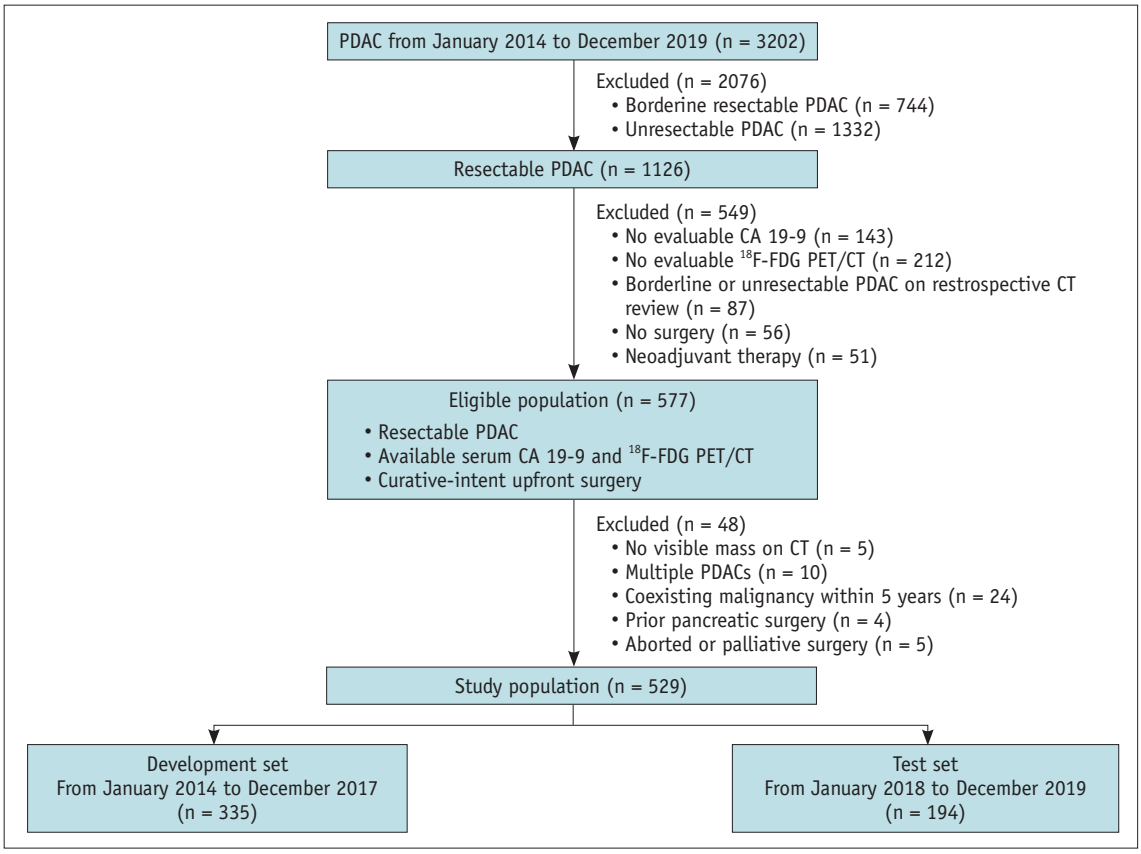

Fig. 1. Flow diagram showing the study population. PDAC = pancreatic ductal adenocarcinoma, CA 19-9 = carbohydrate antigen 19-9, ^{18}F-FDG = fluorine-18-fluorodeoxyglucose

https://doi.org/10.3348/kjr.2023.1235

Table 1. Characteristics of the study population

Characteristic	Development set (n = 335)	Test set (n = 194)	*P*
Mean age, yrs*	64.3 ± 9.3	65.9 ± 9.1	0.05
Sex, male	198 (59.1)	103 (53.1)	0.18
Body mass index, kg/m^2*	23.2 ± 3.2	23.2 ± 3.3	0.82
Laboratory results†			
CA 19-9, U/mL	76.2 (22.2–276.0)	59.6 (17.0–205.6)	0.21
Bilirubin, mg/dL	0.6 (0.4–1.1)	0.5 (0.4–0.8)	0.08
Albumin, g/dL	3.6 (3.3–3.8)	3.6 (3.4–3.8)	0.74
Lymphocyte, 10^9/L	1.8 (1.5–2.3)	1.8 (1.4–2.2)	0.14
Platelet, 10^9/L	223 (186–276)	211 (186.0–252.8)	0.14
Alkaline phosphatase, IU/L	81 (59.5–129.0)	75 (59.3–101.8)	0.10
C-reactive protein, mg/dL	0.1 (0.1–0.5)	0.1 (0.1–0.3)	0.06
Imaging findings			
Tumor size, cm*	2.7 ± 1.0	2.6 ± 0.9	0.37
Dominant tumor location			0.49
Head	204 (60.9)	110 (56.7)	
Body	62 (18.5)	44 (22.7)	
Tail	69 (20.6)	40 (20.6)	
Adjacent organ invasion	102 (30.4)	57 (29.4)	0.80
Tumor SUV_{max}†	5.2 (3.9–7.0)	4.9 (3.5–6.6)	0.36
Suspicious regional LN	84 (25.1)	42 (21.6)	0.37
Possible metastasis on ^{18}F-FDG PET/CT	8 (2.4)	3 (1.5)	0.51
Type of pancreatic resection			0.57
Pancreaticoduodenectomy	202 (60.3)	108 (55.7)	
Distal pancreatectomy	126 (37.6)	81 (41.8)	
Total pancreatectomy	7 (2.1)	5 (2.6)	
Additional resection			
Vein resection	53 (15.8)	21 (10.8)	0.11
Artery resection	8 (2.4)	3 (1.5)	0.51
Metastatectomy	7 (2.1)	2 (1.0)	0.36
Negative resection margin (R0)	258 (77.0)	163 (84.0)	0.05
AJCC pathological tumor stage			0.08
1A	37 (11.0)	35 (18.0)	
1B	96 (28.7)	57 (29.4)	
2A	17 (5.1)	11 (5.7)	
2B	128 (38.2)	73 (37.6)	
3	50 (14.9)	16 (8.2)	
4	7 (2.1)	2 (1.0)	
Follow-up data			
Follow-up duration, mos†	79.0 (66.6–89.8)	42.2 (35.2–49.1)	< 0.001
Recurrence-free survival, mos†	12.0 (5.9–33.4)	14.6 (7.3–31.4)	< 0.001
Overall survival, mos†	33.0 (16.1–61.0)	33.6 (21.1–43.1)	< 0.001

Unless otherwise indicated, data are numbers, with percentages in parentheses.
*Data are expressed as means ± standard deviation, †Data are expressed as medians, with interquartile ranges in parentheses.
CA 19-9 = carbohydrate antigen 19-9, SUV_{max} = maximum standardized uptake value, LN = lymph node, ^{18}F-FDG = fluorine-18-fluorodeoxyglucose, AJCC = American Joint Committee on Cancer

patients (7 and 2 patients in the development and test sets, respectively) underwent pancreatectomy with resection of unexpected metastatic lesions identified during surgery, including localized peritoneal metastasis (n = 5), non-regional LN metastasis (n = 2), and single hepatic metastasis (n = 2). Eleven (2.1%) patients (8 and 3 patients in the development and test sets, respectively) had possible distant metastases on ^{18}F-FDG PET/CT. The decision for

https://doi.org/10.3348/kjr.2023.1235

Korean Journal of Radiology
KJR

surgery in these patients was based on a combination of patient preferences and a multidisciplinary panel's assessment of the likelihood of these findings being truly positive, following a thorough review of all available clinical and imaging data. Details of the possible distant metastases on ^{18}F-FDG PET/CT are shown in Supplementary Table 1. The inter-reader agreement on the CT findings is shown in Supplementary Table 2.

Development and Validation of Prediction Model and Risk Score

Because of its nonlinear association with the log relative hazard of RFS (Supplementary Fig. 1), the tumor SUV_{max} was dichotomized at a cutoff point of 5.2, which was determined to be the optimal cutoff for predicting 1-year RFS. Multivariable Cox proportional hazard analysis revealed five independent predictors for RFS, including tumor size (hazard ratio [HR], 1.29 per 1 cm increment; 95% confidence interval [CI], 1.14–1.45; $P < 0.001$), tumor $SUV_{max} \geq 5.2$ (HR, 1.29; 95% CI, 0.99–1.67; $P = 0.06$), suspicious regional LNs (HR, 1.43; 95% CI, 1.07–1.91; $P = 0.02$), possible distant metastasis on ^{18}F-FDG PET/CT (HR, 2.32; 95% CI, 1.08–4.99; $P = 0.03$), and CA 19-9 (HR, 1.02 per 100 U/mL increment; 95% CI, 1.01–1.04; $P = 0.002$) (Table 2).

A risk-scoring system was developed using a multivariable model (Table 3). The score for each variable was determined by rounding the ratio of the regression coefficient of each variable to that of the suspicious LNs (reference variable), which was defined as a score of 1. The risk score (the sum of the scores for each parameter) ranged from 0 to 8 (Supplementary Table 3). In the development set, the discrimination performance of the risk score in predicting RFS, measured using Harrell's C-index, was 0.63 (95% CI, 0.59–0.66) and remained unchanged after optimism correction at internal validation. In the test set, the risk score showed a C-index of 0.61 (95% CI, 0.56–0.66), similar to that of the postoperative pathological tumor stage (0.64; 95% CI, 0.6–0.69; $P = 0.17$). Calibration curves showed a good correlation between the predicted and actual probabilities of RFS in both the development and test sets (Fig. 2). The calibration slopes did not differ significantly from 1 in either the development (slope, 1.0; 95% CI, 0.7–1.3; $P > 0.99$) or the test (slope, 0.81; 95% CI, 0.41–1.22; $P = 0.37$) sets.

Prognostic Stratification Based on Risk Score

A risk score cutoff value of 2, corresponding to the

Table 2. Univariable and multivariable Cox proportional hazard analyses of postoperative recurrence-free survival in the development set

Parameter	Univariable Cox proportional hazard analysis			Multivariable Cox proportional hazard analysis		
	Regression coefficient	HR (95% CI)	*P*	Regression coefficient	HR (95% CI)	*P*
Age (1-year increment)	0.00	1.00 (0.99–1.02)	0.80			
Sex, male	0.17	1.19 (0.92–1.53)	0.19			
Body mass index (1 kg/m^2 increment)	-0.02	0.98 (0.94–1.02)	0.29			
Tumor size (1 cm increment)	0.31	1.37 (1.22–1.52)	< 0.001	0.25	1.29 (1.14–1.45)	< 0.001
Dominant tumor location			0.30			
Head	0.00	1 (reference)				
Body	-0.10	0.90 (0.65–1.26)	0.55			
Tail	0.20	1.22 (0.89–1.67)	0.21			
Adjacent organ invasion	0.34	1.40 (1.08–1.83)	0.01			
Tumor maximum standardized uptake value ≥ 5.2	0.44	1.55 (1.21–1.99)	0.001	0.25	1.29 (0.99–1.67)	0.06
Suspicious regional lymph node	0.54	1.71 (1.29–2.26)	< 0.001	0.36	1.43 (1.07–1.91)	0.02
Possible distant metastasis on ^{18}F-FDG PET/CT	0.95	2.59 (1.22–5.50)	0.01	0.84	2.32 (1.08–4.99)	0.03
CA 19-9 (100 U/mL increment)	0.03	1.03 (1.02–1.05)	< 0.001	0.02	1.02 (1.01–1.04)	0.002
Bilirubin (1 mg/dL increment)	0.04	1.04 (0.96–1.12)	0.35			
Albumin (1 g/dL increment)	-0.06	0.94 (0.68–1.31)	0.72			
Lymphocyte (1 x 10^9/L increment)	-0.011	0.89 (0.74–1.08)	0.24			
Platelet (1 x 10^9/L increment)	0.00	1.00 (1.00–1.00)	0.80			
Alkaline phosphatase (1 IU/L increment)	0.00	1.00 (1.00–1.00)	0.41			
C-reactive protein (1 mg/dL increment)	0.01	1.01 (0.91–1.11)	0.90			

HR = hazard ratio, CI = confidence interval, ^{18}F-FDG = fluorine-18-fluorodeoxyglucose, CA 19-9 = carbohydrate antigen 19-9

https://doi.org/10.3348/kjr.2023.1235

estimated 1-year RFS probability of 50% (Supplementary Table 3), was used to categorize patients into the low-risk (risk score < 2) and high-risk (risk score ≥ 2) groups, taking into account the observed median RFS of 12 months in the development set. The low-risk group exhibited significantly better RFS than the high-risk group in the test (median, 22.6 vs. 14.2 months; $P = 0.006$) set and showed better overall survival than the high-risk group in the test (median, not reached vs. 32.9 months; $P = 0.001$) set (Fig. 3). Figures 4 and 5 show representative cases from the high- and low-risk groups, respectively.

Table 3. Risk scoring system for predicting recurrence-free survival of resectable pancreatic ductal adenocarcinoma

Parameter	Score
Tumor size, cm	
< 2	0
2–4	1
≥ 4	2
Tumor maximum standardized uptake value	
< 5.2	0
≥ 5.2	1
Suspicious regional lymph node	
No	0
Yes	1
Possible distant metastasis on ^{18}F-FDG PET/CT	
No	0
Yes	2
CA 19-9 level	
< 700	0
700–2400	1
≥ 2400	2

The risk score system was developed using the regression coefficients of the variables calculated in the multivariable Cox proportional hazard model. The score for each variable was calculated by rounding the ratio of the regression coefficient of each variable to that of suspicious regional lymph nodes (reference variable), which was defined as a score of 1. CA 19-9 level was categorized at points of these ratios to be 0.5 and 1.5. CA 19-9 = carbohydrate antigen 19-9, ^{18}F-FDG = fluorine-18-fluorodeoxyglucose

Correlation of Imaging Findings and CA 19-9 with Pathological Findings

The results of comparing tumor SUV_{max} and CA 19-9 with prognostic pathological findings [32] are presented in Supplementary Table 4. A tumor SUV_{max} of ≥ 5.2 was associated with a higher T stage ($P < 0.001$) and poorer tumor differentiation ($P = 0.003$). A higher CA 19-9 levels were associated with higher T stage ($P < 0.001$), LN metastasis ($P = 0.03$), perineural invasion ($P = 0.04$), and lymphovascular invasion ($P = 0.02$). The sensitivity and specificity of suspicious regional LNs for detecting pathological LN metastases were 32.0% (87/272) and 84.8% (218/257), respectively. When only ^{18}F-FDG PET/CT or CT findings were considered, the sensitivities and specificities were 19.5% (53/272) and 92.2% (237/257), respectively, for ^{18}F-FDG PET/CT and 23.5% (64/272) and 89.9% (231/257), respectively, for CT.

DISCUSSION

Despite growing interest in neoadjuvant therapy for treating resectable PDAC, the criteria for selecting high-risk patients with resectable tumors still need to be determined. We identified five independent preoperative factors

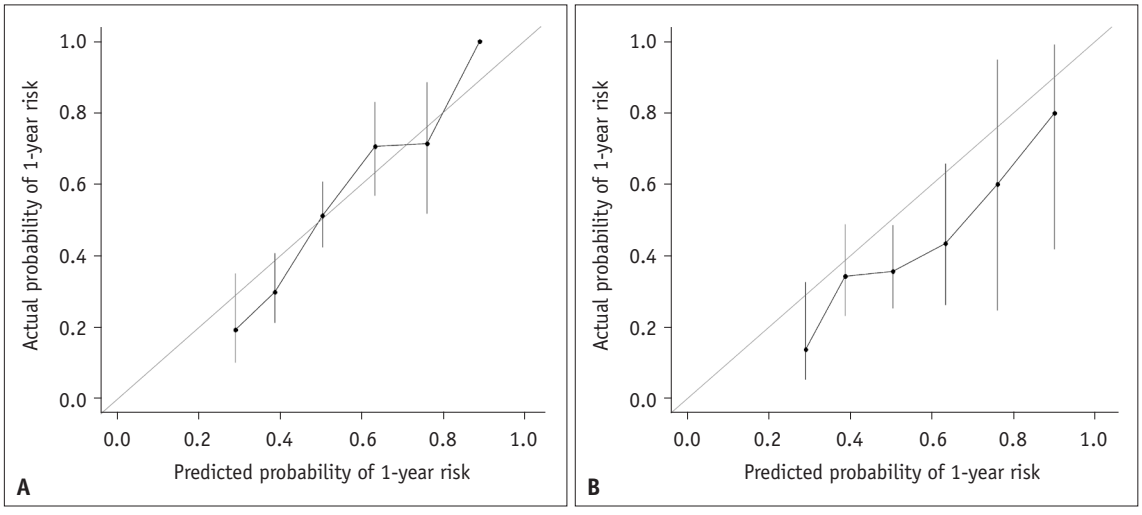

Fig. 2. Calibration plots of the risk score comparing predicted and observed risk of recurrence or death at one year in the development **(A)** and test **(B)** sets.

https://doi.org/10.3348/kjr.2023.1235

Korean Journal of Radiology
KJR

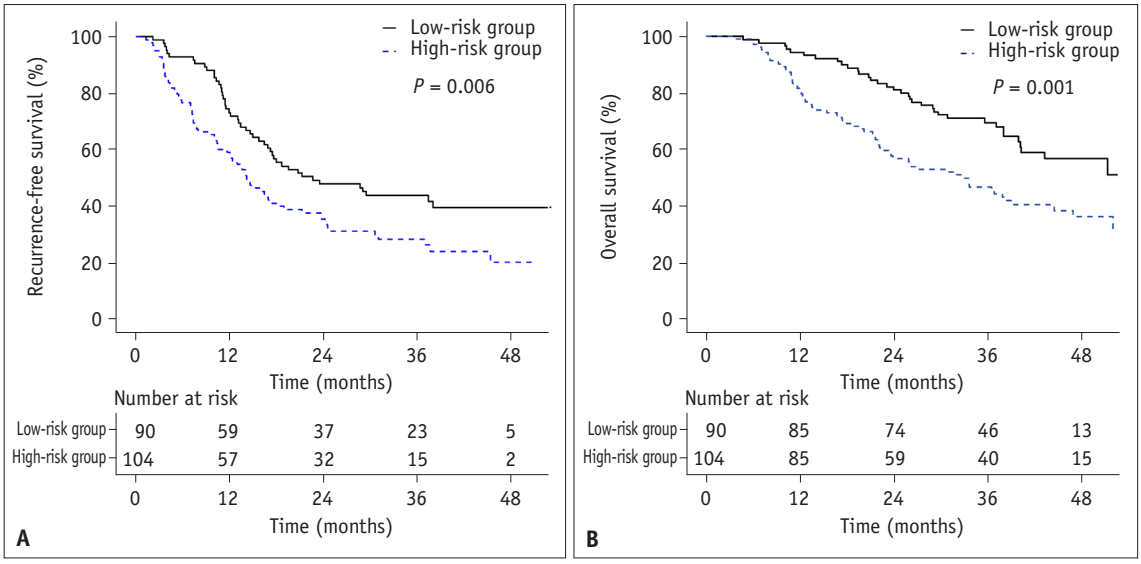

Fig. 3. Recurrence-free survival and overall survival according to risk groups. **A:** Kaplan–Meier curves for the recurrence-free survival of the low-risk and high-risk groups in the test sets. **B:** Kaplan–Meier curves for the overall survival of the low-risk and high-risk groups in the test sets.

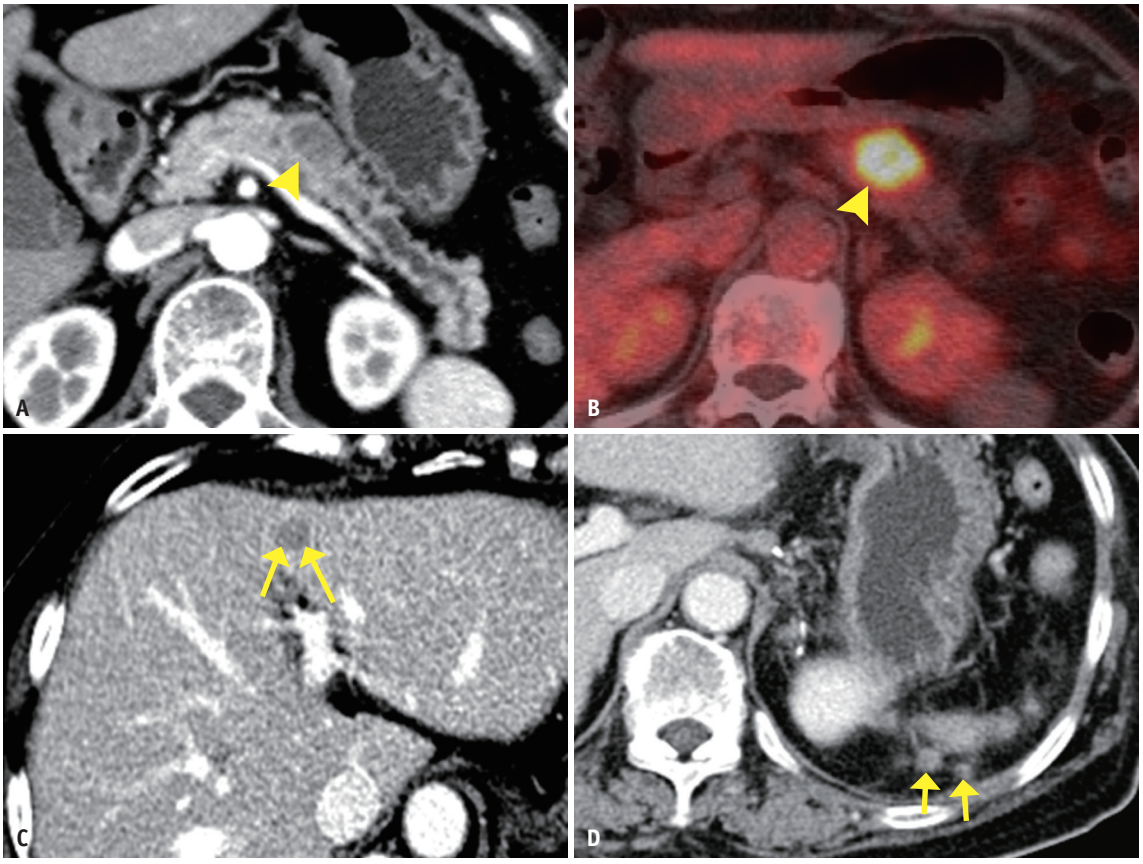

Fig. 4. A 71-year-old female with PDAC was classified into the high-risk group. The pancreatic parenchymal phase of pancreatic protocol CT scan shows a 2-cm biopsy-proven PDAC (arrowheads) in the pancreas tail **(A)** with a SUV_{max} of 7.5 on ^{18}F-FDG PET/CT **(B)**. The CA 19-9 level was 3840 U/mL. The risk score for this patient was 4 points, with 1 point for tumor size, 1 point for SUV_{max}, and 2 points for CA 19-9 level, and she was classified into the high-risk group. The CT scan performed 2.5 months after pancreatic resection reveals metastasis in the liver (arrows) **(C)** and peri-splenic area (arrows) **(D)**. PDAC = pancreatic ductal adenocarcinoma, SUV_{max} = maximum standardized uptake value, ^{18}F-FDG = fluorine-18-fluorodeoxyglucose, CA 19-9 = carbohydrate antigen 19-9

https://doi.org/10.3348/kjr.2023.1235

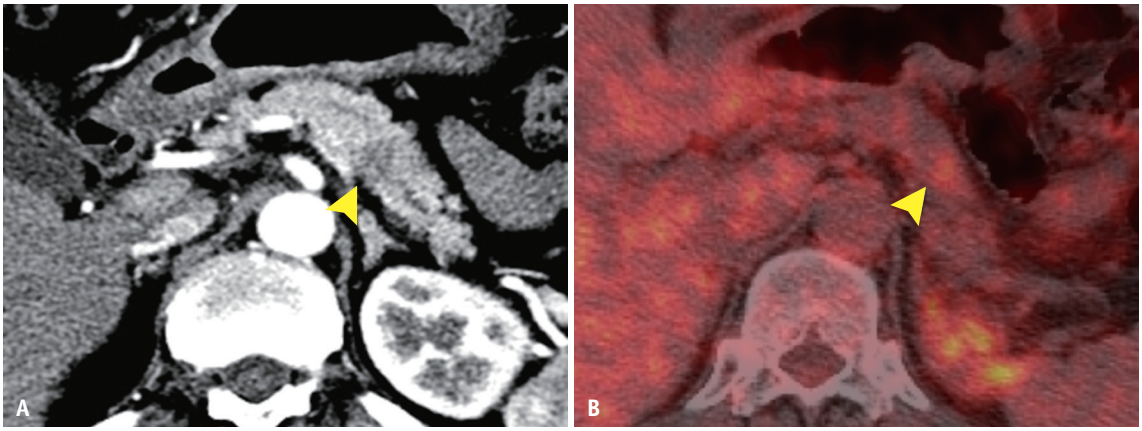

Fig. 5. A 64-year-old male with PDAC was classified into the low-risk group. The pancreatic parenchymal phase of pancreatic protocol CT shows 1.8 cm biopsy-proven PDAC (arrowheads) in the pancreas tail **(A)** with SUV_{max} of 2.7 on ^{18}F-FDG PET/CT **(B)**. The CA 19-9 level was 12 U/mL. No suspicious lymph node or distant metastasis was found on ^{18}F-FDG PET/CT. The patient had a risk score of 0 points and was classified into the low-risk group. The patient remained recurrence-free until 40 months after upfront surgery. PDAC = pancreatic ductal adenocarcinoma, SUV_{max} = maximum standardized uptake value, ^{18}F-FDG = fluorine-18-fluorodeoxyglucose, CA 19-9 = carbohydrate antigen 19-9

predicting postsurgical RFS in patients with this disease: a large tumor size, tumor SUV_{max} of ≥ 5.2, suspicious regional LNs, possible distant metastasis on ^{18}F-FDG PET/CT, and a high CA 19-9 level. The risk score incorporating these factors accurately predicted postsurgical RFS (C-index, 0.61), similar to the postoperative pathological tumor stage (C-index, 0.64) in the test set. It stratified the patients into two groups with different recurrence-free and overall survival rates.

Our study revealed that baseline CA 19-9 levels were independently associated with RFS after upfront surgery in patients with resectable PDAC. The International Association of Pancreatology [7] proposed a CA 19-9 levels > 500 U/mL as a high-risk criterion for anatomically resectable PDAC. However, this criterion needs more solid evidence as most studies on the prognostic implications of CA 19-9 in PDAC have not explicitly focused on resectable PDAC [32-35]. Ushida et al. [8] recently reported that CA 19-9 levels > 500 U/mL were associated with poor overall survival in patients with resectable PDAC. Furthermore, we observed a linear association between CA 19-9 levels and risk of recurrence, with an adjusted HR of 0.02 per 100 U/mL increment of CA 19-9. Thus, we proposed two threshold levels, 700 and 2400 U/mL, to account for the increased risk associated with increasing CA 19-9 levels.

This study found that tumor SUV_{max} was a predictive factor for postsurgical RFS and proposed an optimal cutoff of 5.2 for tumor SUV_{max}. Tumor SUV changes after neoadjuvant therapy in borderline resectable or locally advanced PDAC have prognostic value [36,37]; however, evidence of their role in resectable PDAC is limited. Consistent with our findings, Moon et al. [10] reported that a higher tumor SUV_{max} is associated with poorer overall survival after upfront surgery for resectable PDAC. Unlike Moon et al. [10], which conducted only univariable analysis, we demonstrated the independent predictive value of a tumor SUV_{max} of ≥ 5.2 after adjusting for other factors through multivariable modeling, providing strong evidence of its prognostic role.

Here, the presence of suspicious regional LN detected on ^{18}F-FDG PET/CT or CT was a predictor of postsurgical RFS. Both ^{18}F-FDG PET/CT and CT exhibited low sensitivity (19.5% and 23.5%, respectively) and high specificity (92.2% and 89.9%, respectively) in identifying pathological LN metastasis. To address the low sensitivity of both modalities, we combined the findings of ^{18}F-FDG PET/CT and CT to identify suspicious regional LNs, resulting in a modest improvement in sensitivity (32.0%) and a slight reduction in specificity (84.8%). Despite the low sensitivity of both modalities, the prognostic value of suspicious regional LNs detected using ^{18}F-FDG PET/CT or CT was also recently reported [38]. Taken together, the presence of suspicious regional LN detected using ^{18}F-FDG PET/CT or CT suggests the presence of pathological LN metastasis and a high risk of recurrence in patients with resectable PDAC.

Recurrence was strongly predicted by the presence of distant metastases on ^{18}F-FDG PET/CT. This raises the question of why patients with such findings undergo surgery. During the initial phase of our study, the currently preferred neoadjuvant therapy regimen was unavailable. Furthermore, ^{18}F-FDG PET/CT results were inconclusive and inconsistent with other clinical and imaging findings, leading the

https://doi.org/10.3348/kjr.2023.1235

Korean Journal of Radiology
KJR

multidisciplinary panel to opt for surgery. Our findings suggest that distant metastases on ^{18}F-FDG PET/CT are a justifiable criterion for considering neoadjuvant therapy in patients with otherwise anatomically resectable PDAC.

Our study supports the consensus opinions of the International Association of Pancreatology [7] and the Japanese Society of Hepato-Biliary-Pancreatic Surgery [6], emphasizing the factors reflecting tumor biology, precisely CA 19-9 level and tumor SUV_{max}, in addition to anatomical resectability for treatment selection in patients with PDAC. Our risk score, incorporating these factors, may help select high-risk patients with resectable PDAC who are reasonable candidates for neoadjuvant therapy. Furthermore, the risk score may be used in future clinical trials for neoadjuvant treatment in patients with resectable PDAC to define the inclusion criteria.

Our study had several limitations. First, there were differences in some characteristics between the development and test sets, including more prolonged RFS and OS in the test set than in the development set. These differences may be attributed to the increasing use of neoadjuvant therapy in high-risk patients with resectable PDAC, potentially excluding these patients from the test set enrolled later in the study period. However, these differences may have contributed to the robustness of the test results, reflecting the diversity in real-world practice and avoiding overly optimistic results. Second, our results, obtained from a single high-volume center, may only be generalizable to some institutions; therefore, further external validation of our risk scores is required. Third, we did not consider the Lewis antigen phenotype; the CA 19-9 levels have limited utility in Lewis antigen-negative patients, who account for up to 10% of the general population because they do not express CA 19-9. Lastly, the retrospective design may have introduced selection bias and bias from missing data despite our efforts to minimize it.

In conclusion, we proposed and validated a risk score based on tumor size, CA 19-9 level, SUV_{max}, suspicious regional LNs, and possible distant metastasis on ^{18}F-FDG PET/CT to predict RFS following upfront surgery in patients with resectable PDAC. This risk score may be clinically valuable in selecting high-risk patients with resectable PDAC.

Supplement

The Supplement is available with this article at https://doi.org/10.3348/kjr.2023.1235.

Availability of Data and Material

The datasets generated or analyzed during the study are available from the corresponding author on reasonable request.

Conflicts of Interest

Seung Soo Lee, who holds the respective position of Editorial Board Member of the *Korean Journal of Radiology*, was not involved in the editorial evaluation or decision to publish this article. The remaining author has declared no conflicts of interest.

Author Contributions

Conceptualization: Seung Soo Lee. Data curation: Boryeong Jeong, Minyoung Oh, Seung Soo Lee. Formal analysis: Boryeong Jeong, Nayoung Kim. Funding acquisition: Seung Soo Lee. Investigation: Boryeong Jeong, Minyoung Oh, Seung Soo Lee. Methodology: Seung Soo Lee, Boryeong Jeong. Project administration: Seung Soo Lee. Resources: Jae Seung Kim, Woohyung Lee, Song Cheol Kim, Hyoung Jung Kim, Jin Hee Kim, Jae Ho Byun. Supervision: Seung Soo Lee. Validation: Boryeong Jeong, Minyoung Oh, Seung Soo Lee. Visualization: Boryeong Jeong. Writing—original draft: Boryeong Jeong, Minyoung Oh. Writing—review & editing: Seung Soo Lee.

ORCID IDs

Boryeong Jeong
https://orcid.org/0000-0003-2664-0252
Minyoung Oh
https://orcid.org/0000-0002-6840-3215
Seung Soo Lee
https://orcid.org/0000-0002-5518-2249
Nayoung Kim
https://orcid.org/0000-0002-6504-6590
Jae Seung Kim
https://orcid.org/0000-0003-1710-1185
Woohyung Lee
https://orcid.org/0000-0002-8119-6943
Song Cheol Kim
https://orcid.org/0000-0003-4552-4169
Hyoung Jung Kim
https://orcid.org/0000-0003-3391-5621
Jin Hee Kim
https://orcid.org/0000-0001-5036-3326
Jae Ho Byun
https://orcid.org/0000-0003-2076-9979

Funding Statement

This work was supported by the National Research Foundation of Korea (NRF) grant funded by the Korea government (MSIT) (NRF-2020R1F1A1048826).

REFERENCES

1. Mizrahi JD, Surana R, Valle JW, Shroff RT. Pancreatic cancer. *Lancet* 2020;395:2008-2020
2. Kim DW, Lee SS, Kim SO, Kim JH, Kim HJ, Byun JH, et al. Estimating recurrence after upfront surgery in patients with resectable pancreatic ductal adenocarcinoma by using pancreatic CT: development and validation of a risk score. *Radiology* 2020;296:541-551
3. National Comprehensive Cancer Network. Pancreatic adenocarcinoma, version 2.2022. NCCN clinical practice guidelines in oncology [accessed on June 10, 2023]. Available at: https://www.nccn.org/professionals/physician_gls/pdf/pancreatic.pdf
4. Committee of the Korean Clinical Practice Guideline for Pancreatic Cancer and National Cancer Center, Korea. Korean clinical practice guideline for pancreatic cancer 2021: a summary of evidence-based, multi-disciplinary diagnostic and therapeutic approaches. *Pancreatology* 2021;21:1326-1341
5. Ghaneh P, Palmer D, Cicconi S, Jackson R, Halloran CM, Rawcliffe C, et al. Immediate surgery compared with short-course neoadjuvant gemcitabine plus capecitabine, FOLFIRINOX, or chemoradiotherapy in patients with borderline resectable pancreatic cancer (ESPAC5): a four-arm, multicentre, randomised, phase 2 trial. *Lancet Gastroenterol Hepatol* 2023;8:157-168
6. Oba A, Del Chiaro M, Satoi S, Kim SW, Takahashi H, Yu J, et al. New criteria of resectability for pancreatic cancer: a position paper by the Japanese Society of Hepato-Biliary-Pancreatic Surgery (JSHBPS). *J Hepatobiliary Pancreat Sci* 2022;29:725-731
7. Isaji S, Mizuno S, Windsor JA, Bassi C, Fernández-Del Castillo C, Hackert T, et al. International consensus on definition and criteria of borderline resectable pancreatic ductal adenocarcinoma 2017. *Pancreatology* 2018;18:2-11
8. Ushida Y, Inoue Y, Ito H, Oba A, Mise Y, Ono Y, et al. High CA19-9 level in resectable pancreatic cancer is a potential indication of neoadjuvant treatment. *Pancreatology* 2021;21:130-137
9. Takahashi H, Yamada D, Asukai K, Wada H, Hasegawa S, Hara H, et al. Clinical implications of the serum CA19-9 level in "biological borderline resectability" and "biological downstaging" in the setting of preoperative chemoradiation therapy for pancreatic cancer. *Pancreatology* 2020;20:919-928
10. Moon D, Kim H, Han Y, Byun Y, Choi Y, Kang J, et al. Preoperative carbohydrate antigen 19-9 and standard uptake value of positron emission tomography-computed tomography as prognostic markers in patients with pancreatic ductal adenocarcinoma. *J Hepatobiliary Pancreat Sci* 2022;29:1133-1141
11. Barnes CA, Aldakkak M, Clarke CN, Christians KK, Bucklan D, Holt M, et al. Value of pretreatment 18F-fluorodeoxyglucose positron emission tomography in patients with localized pancreatic cancer treated with neoadjuvant therapy. *Front Oncol* 2020;10:500
12. Moons KG, Altman DG, Reitsma JB, Ioannidis JP, Macaskill P, Steyerberg EW, et al. Transparent reporting of a multivariable prediction model for individual prognosis or diagnosis (TRIPOD): explanation and elaboration. *Ann Intern Med* 2015;162:W1-W73
13. Bosman FT, Carneiro F, Hruban RH, Theise ND. *WHO classification of tumours of the digestive system*. 4th ed. Geneva: World Health Organization, 2010
14. Hong SB, Lee SS, Kim JH, Kim HJ, Byun JH, Hong SM, et al. Pancreatic cancer CT: prediction of resectability according to NCCN criteria. *Radiology* 2018;289:710-718
15. Strijker M, Chen JW, Mungroop TH, Jamieson NB, van Eijck CH, Steyerberg EW, et al. Systematic review of clinical prediction models for survival after surgery for resectable pancreatic cancer. *Br J Surg* 2019;106:342-354
16. Tsen A, Barbara M, Rosenkranz L. Dilemma of elevated CA 19-9 in biliary pathology. *Pancreatology* 2018;18:862-867
17. Kim SS, Lee S, Lee HS, Bang S, Han K, Park MS. Retrospective evaluation of treatment response in patients with nonmetastatic pancreatic cancer using CT and CA 19-9. *Radiology* 2022;303:548-556
18. Al-Hawary MM, Francis IR, Chari ST, Fishman EK, Hough DM, Lu DS, et al. Pancreatic ductal adenocarcinoma radiology reporting template: consensus statement of the Society of Abdominal Radiology and the American Pancreatic Association. *Radiology* 2014;270:248-260
19. Nishiyama Y, Yamamoto Y, Yokoe K, Monden T, Sasakawa Y, Tsutsui K, et al. Contribution of whole body FDG-PET to the detection of distant metastasis in pancreatic cancer. *Ann Nucl Med* 2005;19:491-497
20. Hofman MS, Hicks RJ. How we read oncologic FDG PET/CT. *Cancer Imaging* 2016;16:35
21. Amin MB, Greene FL, Edge SB, Compton CC, Gershenwald JE, Brookland RK, et al. The eighth edition AJCC cancer staging manual: continuing to build a bridge from a population-based to a more "personalized" approach to cancer staging. *CA Cancer J Clin* 2017;67:93-99
22. Campbell F, Cairns A, Duthie F, Feakins R. Dataset for histopathological reporting of carcinomas of the pancreas, ampulla of Vater and common bile duct [accessed on June 10, 2023]. Available at: https://www.rcpath.org/static/34910231-c106-4629-a2de9e9ae6f87ac1/G091-Dataset-for-histopathological-reporting-of-carcinomas-of-the-pancreas-ampulla-of-Vater-and-common-bile-duct.pdf
23. Schafer JL. *Analysis of incomplete multivariate data*. New York: CRC Press, 1997
24. Royston P, Parmar MK. Flexible parametric proportional-hazards

https://doi.org/10.3348/kjr.2023.1235

and proportional-odds models for censored survival data, with application to prognostic modelling and estimation of treatment effects. *Stat Med* 2002;21:2175-2197
25. Bewick V, Cheek L, Ball J. Statistics review 13: receiver operating characteristic curves. *Crit Care* 2004;8:508-512
26. Sullivan LM, Massaro JM, D'Agostino RB Sr. Presentation of multivariate data for clinical use: the Framingham study risk score functions. *Stat Med* 2004;23:1631-1660
27. Chambless LE, Diao G. Estimation of time-dependent area under the ROC curve for long-term risk prediction. *Stat Med* 2006;25:3474-3486
28. Harrell FE Jr, Lee KL, Mark DB. Multivariable prognostic models: issues in developing models, evaluating assumptions and adequacy, and measuring and reducing errors. *Stat Med* 1996;15:361-387
29. van Houwelingen HC. Validation, calibration, revision and combination of prognostic survival models. *Stat Med* 2000;19:3401-3415
30. Crowson CS, Atkinson EJ, Therneau TM. Assessing calibration of prognostic risk scores. *Stat Methods Med Res* 2016;25:1692-1706
31. Pepe M, Longton G, Janes H. Estimation and comparison of receiver operating characteristic curves. *Stata J* 2009;9:1
32. Bilici A. Prognostic factors related with survival in patients with pancreatic adenocarcinoma. *World J Gastroenterol* 2014;20:10802-10812
33. Ferrone CR, Finkelstein DM, Thayer SP, Muzikansky A, Fernandez-delCastillo C, Warshaw AL. Perioperative CA19-9 levels can predict stage and survival in patients with resectable pancreatic adenocarcinoma. *J Clin Oncol* 2006;24:2897-2902
34. Hartwig W, Strobel O, Hinz U, Fritz S, Hackert T, Roth C, et al. CA19-9 in potentially resectable pancreatic cancer: perspective to adjust surgical and perioperative therapy. *Ann Surg Oncol* 2013;20:2188-2196
35. Hess V, Glimelius B, Grawe P, Dietrich D, Bodoky G, Ruhstaller T, et al. CA 19-9 tumour-marker response to chemotherapy in patients with advanced pancreatic cancer enrolled in a randomised controlled trial. *Lancet Oncol* 2008;9:132-138
36. Lee W, Oh M, Kim JS, Park Y, Kwon JW, Jun E, et al. Metabolic activity by FDG-PET/CT after neoadjuvant chemotherapy in borderline resectable and locally advanced pancreatic cancer and association with survival. *Br J Surg* 2021;109:61-70
37. Panda A, Garg I, Truty MJ, Kline TL, Johnson MP, Ehman EC, et al. Borderline resectable and locally advanced pancreatic cancer: FDG PET/MRI and CT tumor metrics for assessment of pathologic response to neoadjuvant therapy and prediction of survival. *AJR Am J Roentgenol* 2021;217:730-740
38. Yoon JK, Park MS, Kim SS, Han K, Lee HS, Bang S, et al. Regional lymph node metastasis detected on preoperative CT and/or FDG-PET may predict early recurrence of pancreatic adenocarcinoma after curative resection. *Sci Rep* 2022;12:17296